

NUCLEAR MEDICINE IMAGING MODALITIES

Radiological imaging modalities such as X-ray radiographic imaging, mammography, and computed tomography (CT) are based on the transmission of X-ray radiation through the body and therefore provide anatomical information about the body. As briefly described in Chapter 1, the anatomical imaging modalities are limited to structural information and do not provide any functional or metabolic information about an organ or a tissue in the body. Since physiological processes are dependent on the metabolic and functional behavior of the tissue, it is important to involve tissue itself in the imaging process. Magnetic resonance imaging (MRI) methods do involve tissue through its chemical composition and therefore are capable of providing some functional and/or metabolic information in addition to anatomical information. However, radionuclide imaging methods directly involve an organ and associated tissue in the body in such a way that the tissue itself becomes a source of radiation that is used in the imaging process. Such methods are also called emission imaging methods and primarily utilize radioactive decay. In the process of radioactive decay, an unstable nucleus disintegrates into a stable nucleus by releasing nuclear energy and emitting photons such as gamma photons and/or specific particles such as positrons and alpha particles (1–5).

6.1. RADIOACTIVITY

A nucleus in an atom contains neutrons and protons. Since protons are positively charged, there is a repulsive force within the nucleus that is also packed with neutrons in a small space. In addition, there are attractive forces between neutrons and protons. The stability of a nucleus depends on the balance of all repulsive and attractive forces within the nucleus. For atomic mass less than 50, nuclei with an equal number of neutrons and protons are usually stable. For atomic mass greater than 50, a higher number of neutrons than protons is required to have a stable nucleus. An unstable nucleus disintegrates through radioactivity in its quest to achieve a stable configuration. The radioactivity is defined as the number of nuclear disintegrations per unit time. The radioactive decay may occur in many ways. However, the decays of significant interest are described below.

- (1) **Alpha Decay:** Decay occurs through emission of alpha (α) particles. An alpha particle, with a typical energy of 4–8 MeV, consists of a helium nucleus with two protons and two neutrons. The penetration of an alpha particle in human tissue is very small, within a few millimeters.
- (2) **Beta Decay:** Beta (β) decay occurs in one of the two ways, either through emission of electrons or through emission of positrons (a positron is a positively charged antiparticle of the electron). Electron emission increases the atomic number by 1 while positron emission decreases the atomic number by 1. The emission of beta particles also ranges a few MeV. Depending on the energy of the beta particle, its penetration in human tissue is also restricted to a few millimeters at the most. Positron emission is particularly interesting and used in the nuclear medical imaging modality called positron emission tomography (PET).
- (3) **Gamma Decay:** Radioactive decay is through the emission of gamma (γ) rays. This type of decay may involve an electron capture process in which an electron from the K- or L-shell is captured by the nucleus, creating a gap in the respective orbit. Electrons from outer shells fill the gap, resulting in emission of characteristic X rays along with γ -rays. Decays by emission of γ -rays with an energy range of 100–200 keV (although higher energy γ -ray photons have also been investigated) are very useful and commonly used for nuclear medical imaging modality in γ -ray imaging or single photon emission computed tomography (SPECT).

Radioactive decay can be described by an exponential decay process with respect to time as

$$N(t) = N(0)e^{-\eta t} \quad (6.1)$$

where $N(0)$ is the number of initial radionuclides, $N(t)$ is the number of radionuclides at time t and η is the radioactive decay constant.

The half-life of a radionuclide decay T_{half} is defined by the time required for half of the radionuclides to transform into stable nuclei, and can be expressed as

$$T_{half} = \frac{0.693}{\eta}. \quad (6.2)$$

As mentioned above, the radioactivity of a radionuclide is defined as the average decay rate that can be computed from the derivative of $N(t)$ with respect to time t and thus is equal to the decay constant times number of $N(t)$. The radioactivity can be measured by one of the two commonly used units: curie or becquerel. A curie (Ci) is equal to the 3.7×10^{10} disintegrations or decays per second (dps). A becquerel (Bq) is equal to one decay per second.

6.2. SPECT

In 1934, Jean Frederic Curie and Irene Curie discovered radiophosphorous ^{32}P , a radioisotope that demonstrated radioactive decay. In 1951, radionuclide imaging of

TABLE 6.1 Gamma Photon Emitter Radionuclides with Their Half-Life Duration and Clinical Applications

Radionuclide	Photon energy (keV)	Half-life (h)	Clinical applications
Technetium ^{99m}Tc	140	6	General and tumor
Thallium ^{201}Tl	135	73	Cardiovascular
Iodine ^{123}I	159	13	Thyroid, tumor
Gallium ^{67}Ga	93, 185, 300, 304	78	Infections
Indium ^{111}In	171, 245	68	Infection, tumor

the thyroid was demonstrated by Cassen through administration of iodine radioisotope ^{131}I (1). Hal Anger in 1952 developed a scintillation camera, later known as the Anger camera, with sodium iodide crystals coupled with photomultiplier tubes (PMTs) (2). Kuhl and Edwards developed a transverse section tomography gamma-ray scanner for radionuclide imaging in the early 1960s (3). Their imaging system included an array of multiple collimated detectors surrounding a patient with rotate-translation motion to acquire projection for emission tomography. With the advances in computer reconstruction algorithms and detector instrumentation, gamma-ray imaging now known as SPECT is used for 3-D imaging of human organs, extended even to full body imaging. Radioisotopes are injected into the body through administration of radiopharmaceutical drugs, which metabolize with the tissue, making the tissue a source of gamma-ray emissions. The gamma rays from the tissue pass through the body and are captured by the detectors surrounding the body to acquire raw data for defining projections. The projection data is then used in reconstruction algorithms to display images with the help of a computer and high-resolution displays. In SPECT imaging, the commonly used radionuclides are thallium (^{201}Tl), technetium (^{99m}Tc), iodine (^{123}I), and gallium (^{68}Ga). These radionuclides decay by emitting gamma rays for imaging with photon energies up to a few hundreds of keV (4–11). Table 6.1 shows the photon energy and half-life of the radioactivity decay for radionuclides used in SPECT imaging.

The attenuation of gamma rays is similar to that of X rays and can be expressed as:

$$I_d = I_0 e^{-\xi x} \quad (6.3)$$

where I_0 is the intensity of gamma rays at the source, I_d is the intensity at the detector after the gamma rays have passed the distance x in the body and a linear attenuation coefficient that depends on the density of the medium, and ξ is the energy of gamma-ray photons.

The radionuclides required for SPECT such as technetium are artificially generated with appropriate radiopharmaceuticals suitable for administration in the body. After the tissue or organ to be imaged becomes radioactive, the patient is positioned in a scanner with detectors placed surrounding the patient. In modern scanners, the detectors are placed in a ring surrounding the patient covering a full 360-degree range. However, scanners involving a finite array of detectors with

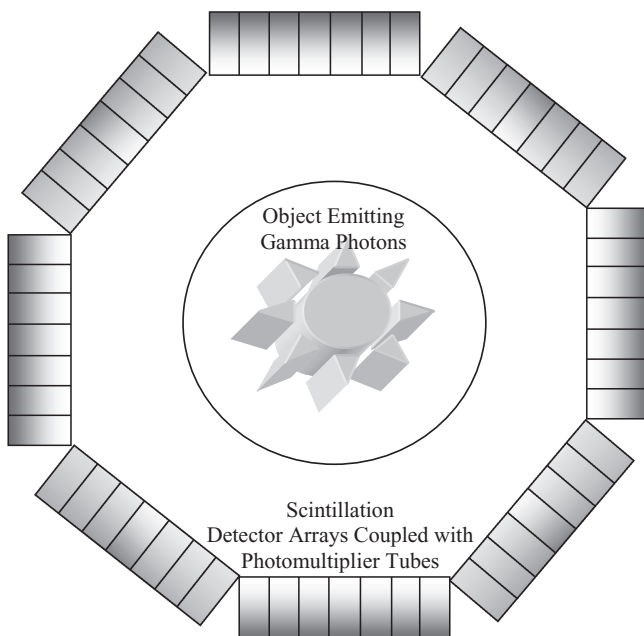


Figure 6.1 A schematic diagram of detector arrays of SPECT scanner surrounding the patient area.

rotational motion are also used. Figure 6.1 shows a schematic representation of a SPECT scanner.

6.2.1 Detectors and Data Acquisition System

The SPECT imaging systems used today are based on the Anger scintillation camera (8), which uses a collimator to reject scatter events and maps scintillation events on the attached scintillation crystal. The scintillation material converts γ -ray photon energy into light photons that are received by a photocathode of a position-sensitive PMT, which converts light photons into electrons that are amplified through a series of dynodes (as described in Chapter 4).

Finally, an amplified electrical voltage signal is digitized using an analog-to-digital convertor and stored in a computer memory with the information about the energy magnitude and position of the detected γ -ray photon. This basic principle is illustrated with details in Figure 6.2.

As illustrated in Figure 6.2, γ -ray photons are emitted from the tissue with the uptake of a radioactive pharmaceutical such as ^{99m}Tc . The emission distribution is isotropic in 3-D space around the patient body. The direct straight-line path between the emission source and detector is important to determine the point of emission for image reconstruction. Not all photons that reach the detector come directly from the emission source of tissue. As shown in Figure 6.2, photon 1 is not detected by the camera as it is not in the direction of the detector. Photon 2 is absorbed within

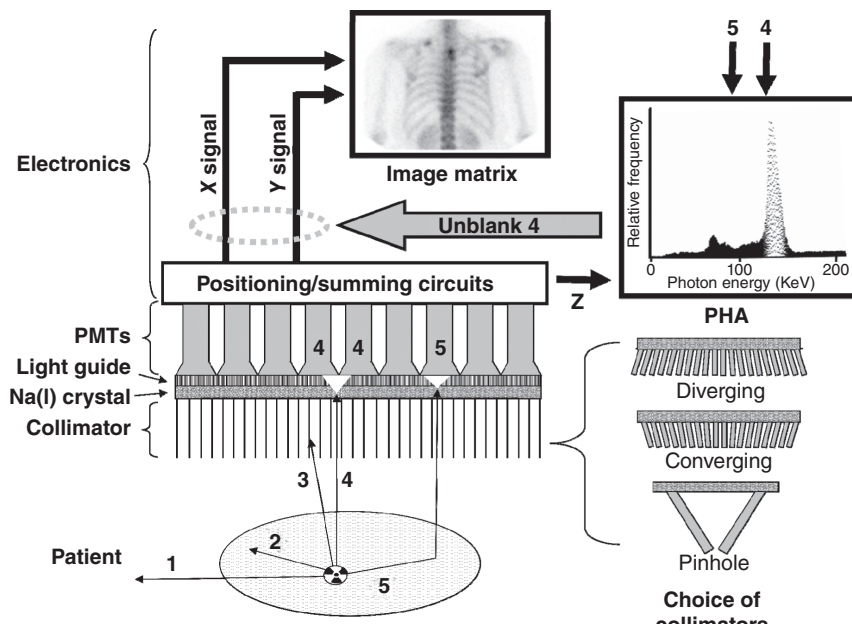


Figure 6.2 A detailed schematic diagram of SPECT imaging system (used with permission from L.S. Zuckier (11); Dr. Lionel Zuckier is gratefully acknowledged).

the body. Photon 3 intersects the detector at an angle other than parallel to the collimator and therefore gets absorbed by the lead septa (walls) of the parallel-hole collimator. Photon 4 travels in a direction such that it is able to pass through a collimator aperture and is detected by the Na(I) scintillation crystal. The energy of the photon is transformed to visible light photons that are received by PMTs, which produce an electronic pulse that is amplified and then analyzed by the positioning and summing circuits to determine the apparent position of scintillation. Figure 6.3 shows a matrix of 8×8 PMTs that are connected with horizontal and vertical summing networks X^+ , X^- , Y^+ , and Y^- , as originally designed by Hal Anger (8). The position of the scintillation event can be detected by analyzing the location of the pulse height in each of the summing network outputs. For example, as shown in Figure 6.3, the scintillation event in box (3,2) will provide higher output current in Y^+ and X^- than in X^+ and Y^- at respective locations since the scintillation event is closer to top (Y^+) and left (X^-) summing networks. The four composite outputs of the summing networks are appropriately amplified and then summed together to provide the total electric current that is converted into respective voltage signal Z . The amplitude of the voltage signal Z is proportional to the energy of the scintillated photon. A pulse-height analyzer (PHA) circuit then examines the amplitude of the voltage signal Z to determine whether to accept and store it in the data matrix or reject it. If the total energy as represented by the amplitude of voltage Z signal (as shown in Fig. 6.2 for photon 4) falls within the full width at half maximum (FWHM) of the energy spectrum of the γ -ray emission of the radioisotope (such as ^{99m}Tc), the scintillation event is accepted and data are stored with its energy level and X-Y

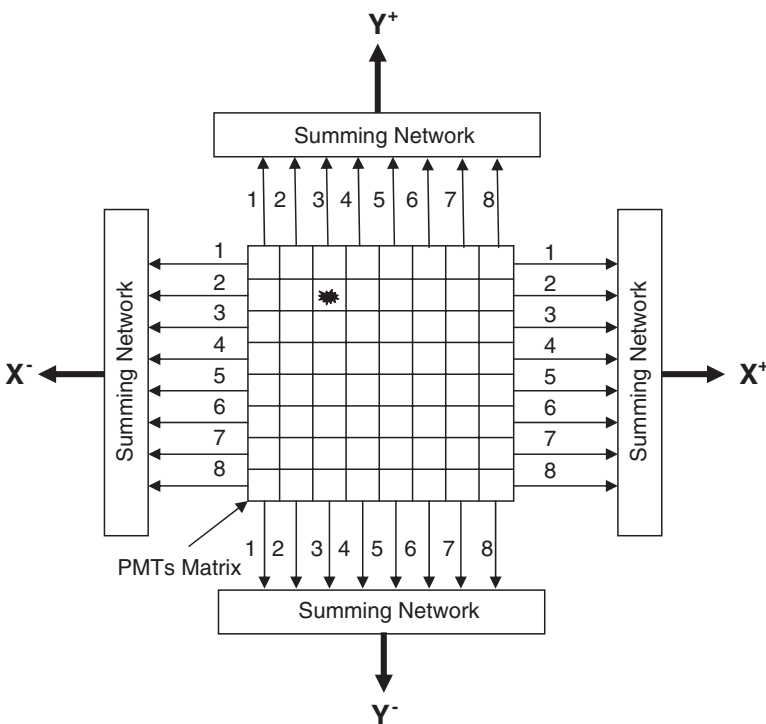


Figure 6.3 A schematic diagram of PMT matrix and summing networks for localization of scintillation events in SPECT imaging systems.

position coordinate information. For ^{99m}Tc radioisotope-based imaging, usually a window of 20% centered on the 140 keV energy peak is used to accept a scintillation event. If a γ -ray photon is scattered within the patient as shown by photon 5 in Figure 6.2, the lower energy of its pulse will cause its rejection by PHA, and the photon will not be included in the data matrix. Parallel-hole collimators are most common in nuclear medicine imaging systems. However, diverging, converging, or pin-hole collimators may be used in place of the parallel-hole collimator as shown in Figure 6.2 to focus on imaging various types and shapes of tissue and organs. The length of the septa of collimator L and the distance d between the septa, and distance Z between the source and the front of the collimator determine the spatial resolution R in the acquired image as

$$R = \frac{d(L + Z)}{L}. \quad (6.4)$$

As can be seen from the above equation, the spatial resolution is improved if the length of the collimator is increased and the detectors are brought closer to the emission source, in other words, closer to the body.

Sodium iodide NaI(Tl) crystal-based scintillation detectors coupled with PMTs are most commonly used for detection of gamma rays to acquire raw data.

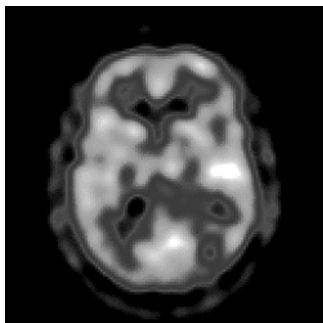


Figure 6.4 A $^{99}\text{m}\text{Tc}$ SPECT image of a human brain.

Other detector material such as barium fluoride (BaF_2), cesium iodide ($\text{CsI}(\text{TI})$), and bismuth germinate (BGO) have also been used for scintillation. After the detection of gamma photons, the projection data is assembled from the raw data and fed into the computerized 3-D reconstruction algorithms. The reconstructed images are displayed on display terminals. Figure 6.4 shows an axial $^{99\text{m}}\text{Tc}$ SPECT image of a human brain. Note that SPECT images are poor in resolution and anatomical structure as compared with CT or MR images. The SPECT images show metabolism information related to a radioactive tracer with specific photon energy. Recently, multiple photon energy imaging has been found very useful in clinical diagnostic radiology by using a single radioisotope that can emit multiple γ -ray energy photons or more than one radioisotope with different γ -ray photon energy emissions. For example, gallium (^{67}Ga) can provide γ -ray photons at 93, 185, 300, and 394 keV (Table 6.1). This becomes possible because of the wide spectral response of scintillation detectors and appropriate PHA. Dual radioisotopes can be used in the body if there is a significant difference in the way they metabolize with the tissue and provide different γ -ray photon energies (11, 12). For example, one can be targeted at metastases while the other could provide information about specific infections in the body. Figure 6.5 shows a dual energy full body scan of the same patient using $^{99\text{m}}\text{Tc}$ and ^{111}In radioisotopes. Two scans specifically provide different information about the marrow and infection in the body.

6.2.2 Contrast, Spatial Resolution, and Signal-to-Noise Ratio in SPECT Imaging

The contrast of SPECT images depends on the signal intensity, which depends on the emission activity of the source. The source intensity is based on the dose, metabolism, and absorption in the body, and the half-life of the radionuclide used for imaging. Low photon statistics and scattering are major problems associated with SPECT imaging. Scattering events cause loss of source information as it is difficult to identify the path of travel for the photon originating from the source. Lead-based collimators are used to reduce detection of scattered events to improve the signal-to-noise ratio (SNR) and detection of actual radiation from the localized source. As described above, the spatial resolution is determined by the design of the

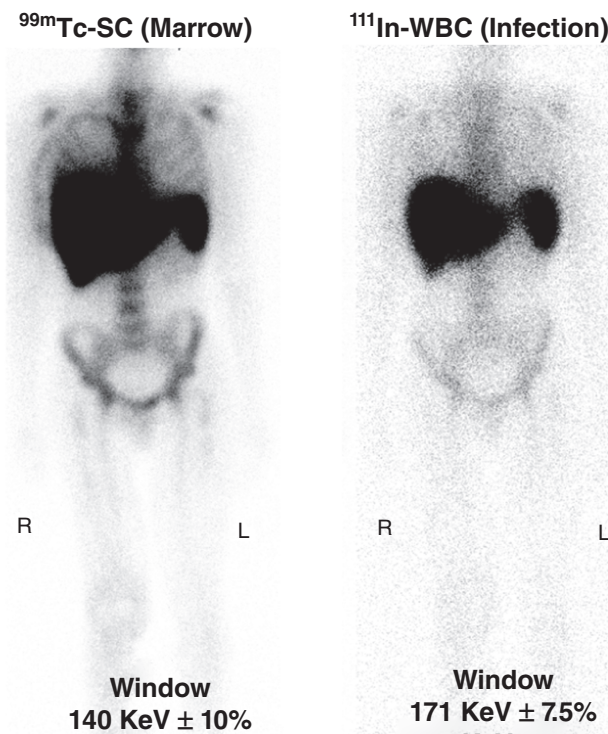


Figure 6.5 Dual-isotope acquisition: 24 h prior to imaging, 0.5 mCi of ^{111}In -labeled autologous white blood cells (^{111}In -WBCs) were injected intravenously into the patient to localize sites of infection. Thirty minutes prior to imaging, 10 mCi of $^{99\text{m}}\text{Tc}$ -sulfur colloid were injected intravenously to localize marrow. Co-imaging of the $^{99\text{m}}\text{Tc}$ window ($140 \pm 20\%$ keV) and dual ^{111}In windows ($171 \pm 15\%$ keV and $245 \pm 15\%$ keV) was performed, thereby producing simultaneous images of the marrow (left panel) and WBC distribution (right panel). Marrow, liver, and spleen are visible on both marrow and WBC studies. The $^{99\text{m}}\text{Tc}$ study is used to estimate WBC activity that is due to normal marrow distribution and of no pathologic consequence. To signify infection, ^{111}In -WBC activity must be greater than the visualized marrow distribution. (Dr. Lionel Zuckier, Director of Nuclear Medicine, University of Medicine and Dentistry of New Jersey, Newark, is gratefully acknowledged for providing the above images (11)).

collimator (septa length and diameter for circular parallel channels) and the distance between the source and collimator. This is the reason that images taken from one direction may not have the same image quality and resolution as an image taken from the opposite side when the source object is not in the middle. The images taken from the direction providing closer distance between the source object and collimator will provide better resolution and image quality.

The SNR depends on signal intensity (source activity as reflected by the dose), tissue metabolism or uptake, total time over which the data are acquired, attenuation within the body, scatter rejection, and detector sensitivity and efficiency.

The nonlinearities caused by the detectors and PMTs make the SPECT imaging process spatially variant. Thus, images would show degradations and geometric artifacts such as cushion and barrel artifacts because the registered detector count fluctuates from the actual count depending on the detector location. Usually, intensity nonuniformities are corrected by using phantom data of uniform emission activity in the region of imaging. The geometric artifacts are difficult to correct, as these corrections require statistical preprocessing methods such as maximum likelihood estimation. Assessment of point spread and line spread functions help in developing preprocessing methods to compensate for detector nonlinearities and sensitivity variations due to geometrical configuration.

Since the source of radiation is inside the body, the gamma photons interact with the matter inside the body for attenuation and scattering processing, including photoelectric absorption and Compton scattering. Such interactions lead to the loss of a photon or significant changes in its direction, in case of Compton scattering events. The distribution of the data (gamma photons) collected by the array of detectors from spatial locations within an object may be different from the actual distribution of emission source activity within the object. The attenuation correction methods incorporate weighting factors that are based on the average regional or pixel-level activity. The scatter correction methods are based on estimation techniques using photon statistics derived from distribution models or experimental measurements. The distribution model-based estimation methods involve Monte Carlo simulations and are computationally expensive. Experimental measurement methods involving comparison of photon counts collected by detectors at different times with different activity levels are commonly used. Figure 6.6 shows the reconstructed SPECT ^{99m}Tc axial images without attenuation correction (left) and with attenuation correction (right) of a brain. The improved structure visibility is evident in the image with attenuation correction while the image without attenuation correction has significant

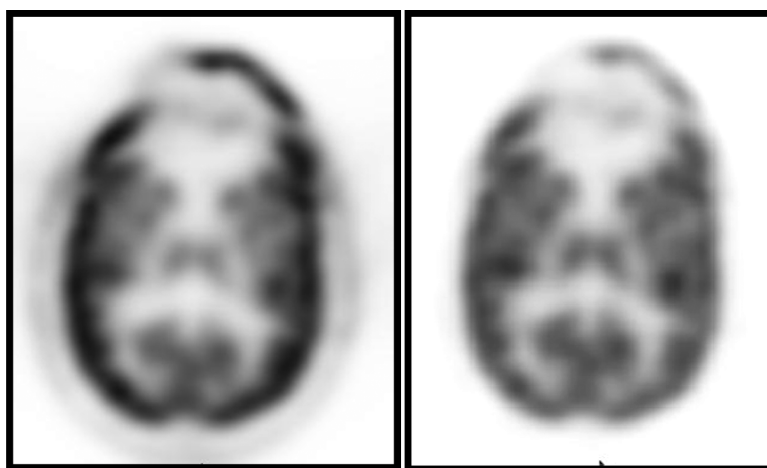


Figure 6.6 SPECT images of a brain reconstructed without attenuation correction (left) and with attenuation correction (right).

blurring of edges. Image reconstruction and estimation algorithms are described in Chapter 8.

Even though SPECT images are poor in structural information because of attenuation and scattering problems, they show important biochemical information tagged with specific physiology. SPECT imaging is a proven tool in the assessment of metastases or characterization of a tumor. Also, SPECT imaging is a low-cost imaging modality compared with PET because of the lower preparation cost of the radioisotopes used in SPECT imaging.

6.3. PET

Positron emission tomography imaging methods were developed in 1970s by a number of researchers including Phelps, Robertson, Ter-Pogossian, and Brownell (9–13). The concept of PET imaging is based on the simultaneous detection of two 511 keV energy photons traveling in the opposite direction. The distinctive feature of PET imaging is its ability to trace radioactive material metabolized in the tissue to provide specific information about its biochemical and physiological behavior.

Some radioisotopes decay by emitting positively charged particles called positrons. Table 6.2 shows some commonly used positron-emitting radionuclides and their half-life duration. The emission of a positron is accompanied by a significant amount of kinetic energy. After emission, a positron travels typically for 1–3 mm, losing some of its kinetic energy. The loss of energy makes the positron suitable for interaction with a loosely bound electron within a material for annihilation. The annihilation of the positron with the electron causes the formation of two gamma photons with 511 keV traveling in opposite directions (close to 180 degrees apart). The two photons can be detected by two surrounding scintillation detectors simultaneously within a small time window. This simultaneous detection within a small time window (typically on the order of nanoseconds) is called a coincidence detection, indicating the origin of annihilation along the line joining the two detectors involved in coincidence detection. Thus, by detecting a large number of coincidences, the source location and distribution can be reconstructed through image reconstruction algorithms. It should be noted that the point of emission of a positron is different from the point of annihilation with an electron. Although the imaging process is aimed at the reconstruction of source representing locations of emission of positrons, it is the locations of annihilation events that are reconstructed as an

TABLE 6.2 Positron Emitter Radionuclides and Their Half-Life Duration

Positron emitting radionuclides	Two-photon energy (keV)	Half-life time (min)
Fluorine ¹⁸ F	511	109
Oxygen ¹⁵ O	511	2
Nitrogen ¹³ N	511	10
Carbon ¹¹ C	511	20

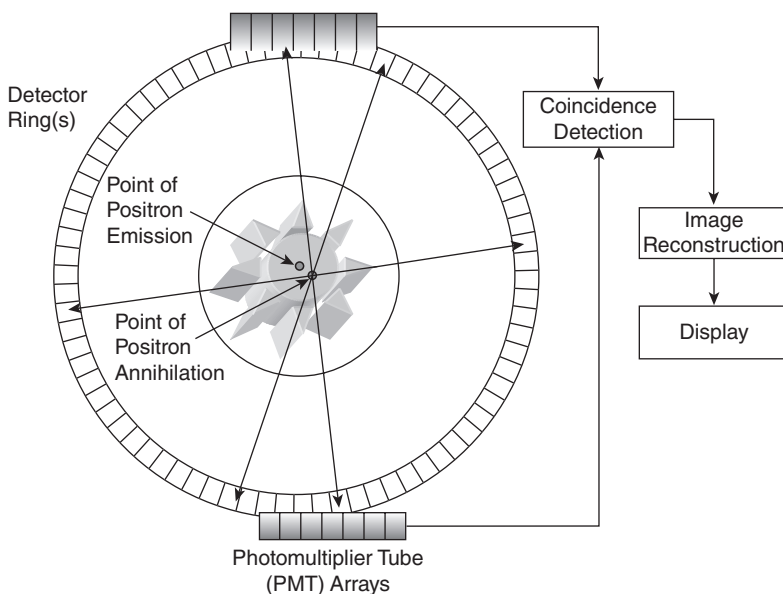


Figure 6.7 A schematic diagram of a PET imaging system.

image in the PET. However, the distribution of emission events of positrons is considered close enough to the distribution of annihilation events within a resolution limit.

As shown in Figure 6.7, coincidence detection forms the basic raw data in PET imaging. The finite time window used in coincidence detection involving two surrounding detectors placed opposite to each other provides an efficient mechanism of electronic collimation. Since the scattered photons have to travel a longer path, they may not reach the detector within a specified time window. Thus, the scattered radiation is likely to be rejected if the coincidence detection time window is appropriately set. Nevertheless, lead-based collimators are also used to reject scattered photons with an angular trajectory. Scintillation detectors coupled with PMTs are used in a single or multiple circular rings surrounding the patient for data acquisition. Commonly used scintillation detectors include sodium iodide ($\text{NaI}(\text{TI})$), barium fluoride (BaF_2), cesium iodide ($\text{CsI}(\text{TI})$), and bismuth germinate (BGO) crystals, but recently semiconductor detectors have also been used in PET imaging scanners.

The main advantage of PET imaging is its ability to extract metabolic and functional information of the tissue because of the unique interaction of the positron with the matter of the tissue. The most common positron emitter radionuclide used in PET imaging is fluorine (^{18}F), which is administered as fluorine-labeled radiopharmaceutical called fluorodeoxyglucose (FDG). The FDG images obtained through PET imaging show very significant information about the glucose metabolism and blood flow of the tissue. Such metabolism information has been proven to be critical in determining the heterogeneity and invasiveness of tumors. Figure 6.8 shows a set of axial cross-sections of brain PET images showing glucose

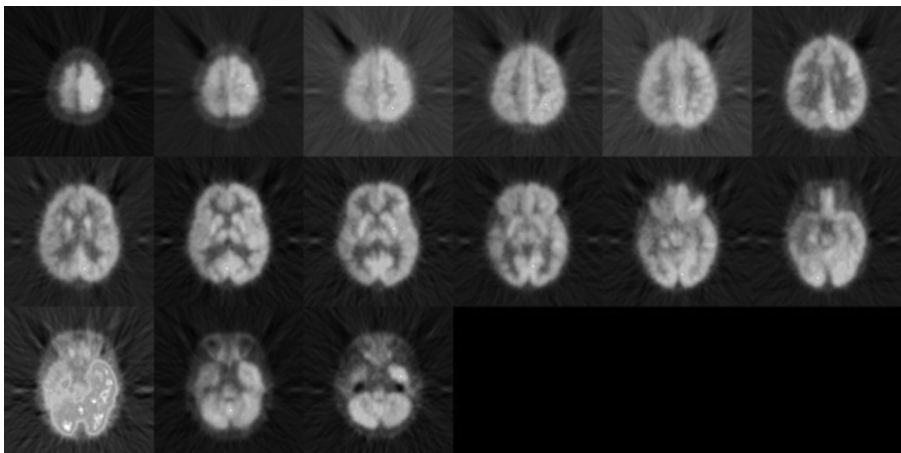


Figure 6.8 Serial axial images of a human brain with FDG-PET imaging.

metabolism. The streaking artifacts and low-resolution details can be noticed in these images. The artifacts seen in PET images are primarily because of the low volume of data caused by the nature of radionuclide–tissue interaction and electronic collimation necessary to reject the scattered events.

6.3.1 Detectors and Data Acquisition Systems

Since the coincidence detection method provides an excellent method of electronic collimation, the degradation effects of scattering are reduced in the data collection process. However, random coincidence and scatter coincidences can still degrade the data, causing poor quality images. The time window for the coincidence detection can be tightened to reduce random coincidences. Another method to reject scattered photons in the coincidence detection is the use of minimum energy level criteria. The scattered photons are of lower energy levels. By applying a threshold to the photon's energy level, photons with lower energy are considered to be coming from scattering interactions and are therefore not included in the coincidence detection. Since the photon's energy level is higher in PET imaging than in SPECT imaging, the attenuation problems in PET imaging are less severe. Several geometrical configuration-based ad hoc correction methods are used in PET imaging. A transmission scan can also be used for a more accurate attenuation correction. The transmission scan can be obtained by using an external positron source for imaging. However, such methods are often sensitive to statistical noise.

6.3.2 Contrast, Spatial Resolution, and SNR in PET Imaging

Contrast, spatial resolution, and sensitivity of PET imaging are significantly better than SPECT imaging mainly because of electronic collimation provided by the coincidence detection method. The coincidence detection method provides a more sensitive and accurate count of the photon-emission events. In addition, resolution

of PET images does not depend on the distance between the emission source and detector. The time window (usually 6–12 ns) can be adjusted to sensitize to the coincidence detection response. A larger time window will allow greater data statistics but at the expense of higher random coincidences. A narrow energy range in the PHA will decrease the scattered photons to be detected in coincidences and provide higher sensitivity to detection of true emission events. However, it will also reduce the number of coincidence events detected by the system, causing a lower amount of data. The pair of 511 keV photons interacts with the body matter in a different way from lower energy photons in SPECT, providing less attenuation. But the spatial resolution is inherently limited by the distance between the emission of positron and its annihilation that emits two 511 keV photons. The SNR is superior in PET images to SPECT but is still affected by the detector efficiency, intensity distribution of source emission, and dose of the positron emitter nuclide. In addition, the SNR is further improved by using retractable septa of the external collimator in multislice imaging when multiple rings of detectors are used. Each detector ring with extended septa receives data directly only from respective parallel planes of slices. This mode rejects any cross-plane event detection, reducing the data to only true coincidence events within the selected plane without any scattering. When the septa are retracted to a specific position, cross-plane events can be allowed. In a full 3-D multi slice imaging mode, the septa may be completely removed to allow cross-planar data acquisition. It should be noted that the removal of septa would provide high sensitivity but with the acceptance of more scattered events, which would impact the spatial resolution.

The most significant advantage of PET imaging is the ability to tag a very specific biochemical activity and trace it with respect to time. PET imaging is an effective radiological imaging tool in metabolic, blood-flow, functional, and neuro-receptor imaging. However, the preparation of radiopharmaceuticals used in PET imaging is much more expensive than those used in SPECT imaging. Also, due to the limitations on detector size and sensitivity, and low emission statistics, the reconstructed images are relatively noisy and poor in resolution compared with MR and CT imaging modalities.

6.4. DUAL-MODALITY SPECT-CT AND PET-CT SCANNERS

X-ray CT and nuclear medicine imaging modalities (SPECT and PET) provide complimentary anatomical and metabolic information about the tissues and organs in the body. For several years patients have been scanned individually in both scanners at different times. Anatomical images from X-ray CT and metabolic images from SPECT or PET have been fused through postprocessing image registration methods using fiducial or internal landmarks. Multimodality image fusion has allowed examination of the metabolism and blood perfusion within an anatomically labeled tissue volume. This is an extremely important issue in diagnostic, treatment, and therapeutic evaluations. However, postprocessing image registration and fusion methods (described in Chapter 12) are not guaranteed to be completely accurate with



Figure 6.9 A picture of Philips Precedence SPECT–Xray CT scanner.

limitations on spatial and contrast resolutions. Recent advances in detector instrumentation, fast data acquisition, and high-capacity storage capabilities have led to hybrid or dual-modality imaging scanners combining SPECT or PET with X-ray CT systems. In these hybrid systems, the γ -ray camera and CT scanner share the same gantry to allow scanning of the patient efficiently by both modalities providing registered sets of X-ray and nuclear medicine images. The registered images can be displayed for any cross-sectional view and through a fused color display, providing visualization of both anatomical and metabolic information. For example, intensity of the gray scales in the fused image can be provided from X-ray anatomical images, but the color shades can be coded with metabolic information. In addition to the availability of accurately registered image sets, the dual-modality imaging system also provides accurate data for attenuation correction from the CT scan to be used in the reconstruction of SPECT or PET images improving their contrast resolution and sensitivity. Furthermore, a dual-modality scanner saves time and health care costs as the patient does not have to be moved or rescheduled for another scan.

Figure 6.9 shows a picture of the Philips Precedence SPECT–X-ray CT imaging system with a flexible γ -ray camera and 16-slice X-ray CT scanner. The Precedence imaging system with 16-slice high-resolution CT and complementary SPECT capabilities provides combined coronary computed tomography angiography (CTA), coronary calcium scoring, and attenuation-corrected SPECT myocardial perfusion imaging in a single imaging session. The accuracy of radionuclide therapy planning using the dual-modality scanners has been widely investigated and claimed to be improved by using the CT attenuation-corrected SPECT data. A wide spectrum of clinical applications includes combined coronary CT angiography and myocardial perfusion imaging.

Figure 6.10 shows a SPECT image (on the left), a CT image (in the middle), and a fused SPECT–CT image of a human brain. It is evident that the metabolic

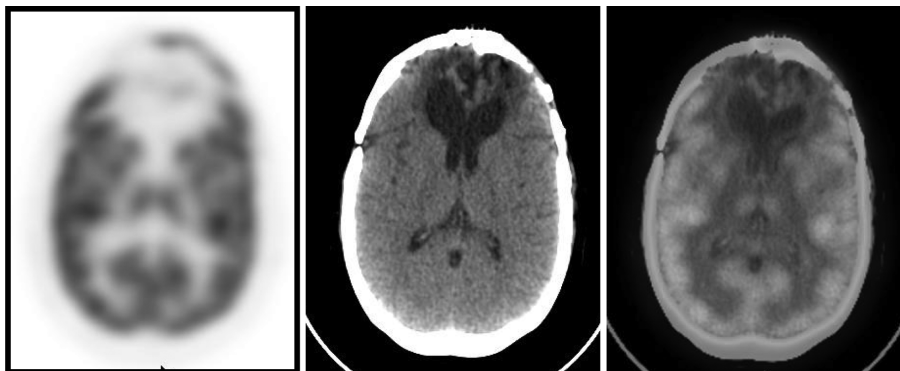


Figure 6.10 A ^{99m}Tc SPECT image (left), X-ray CT image (middle), and the fused SPECT-CT image (right) of the same axial section of a brain.



Figure 6.11 A picture of Philips GEMINI TF Big Bore PET-CT imaging system.

information in anatomical cortical structures can be better examined and evaluated from the fused image.

Philips dual-modality PET-CT GEMINI imaging system (shown in Fig. 6.11) provides a combined multislice advanced PET imaging with high-resolution X-ray CT using the same large gantry with 85 cm bore diameter. The dual-modality imaging technology allows consolidation of radiation oncology procedures with better accuracy and scheduling. The PET imaging scanner in the GEMINI system also uses time-of-flight (TOF) information in iterative reconstruction methods for better quality reconstructed images. During the coincidence detection when two photons are detected in two detectors across the line of coincidence, the time interval between the detections with their respective order of detection is called TOF information. If an annihilative event is closer to one detector than the other along the line of coincidence, the photon detection in the nearest detector is followed by the second

detection event in the farthest detector with a longer delay. If the annihilation is in the middle of line of coincidence, both photons will reach their respective detectors at almost the same time, giving a very short time interval between two detection events. Thus TOF information can be used in estimating the point of photon emission (annihilation event) along the line of coincidence to improve the sensitivity, spatial resolution, and quality of reconstructed images. Advantages of dual-modality Philips PET-CT imaging system include automatic registration, image fusion, and tracking of anatomically labeled segmented regions of specific metabolism. It also provides a seamless data transfer capability to radiation treatment and planning systems. The dual-imaging capability improves patient scheduling and lowers health care costs.

6.5. EXERCISES

- 6.1. What are the principles of SPECT and PET imaging modalities?
- 6.2. How γ -ray photons are generated by a radioisotope?
- 6.3. Why do some radionuclides such as ^{67}Ga produce multiple energy γ -rays? Describe the emission spectra of ^{67}Ga .
- 6.4. Assume that a radioisotope reduces its radioactivity by 1/3 every hour. What is the decay constant?
- 6.5. What is the advantage of dual-energy photon SPECT imaging?
- 6.6. What scintillation detectors are used in SPECT imaging?
- 6.7. Describe the function of Anger's summing networks for position and pulse-height analysis.
- 6.8. A parallel-hole collimator is designed to have 4 mm diameter holes with the 8 mm long septa. Find the maximum spatial resolution if the distance between the body of the patient and front of the collimator is 10 cm.
- 6.9. Find and compare the spatial resolution, if the distance between the body of the patient and front of the collimator is (a) reduced to 4 cm, and (b) increased to 13 cm.
- 6.10. Find the spatial resolution of a pin-hole collimator with a front hole of 4 mm diameter, 8 mm long septa, and 10 cm distance between the patient body and the pinhole.
- 6.11. Find the impact on the spatial resolution if there is a 1.5 mm gap between the back of the septa and front of the scintillation crystal.
- 6.12. What are the advantages of PET over MRI and fMRI modalities?
- 6.13. Describe the advantages and disadvantages of PET over SPECT.
- 6.14. Describe the relationship among the detector size, signal-to-noise ratio, and image resolution for SPECT and PET imaging modalities.
- 6.15. What should be the preferred characteristics of a detection system in PET imaging modality?

- 6.16. What is time-of-flight information in PET imaging and how can it help in improving image quality?
- 6.17. Display ^{99m}Tc -SPECT and MR brain images for the same axial slice in MATLAB. Apply edge enhancement methods to both images and compare the definitions of the cortical structure in SPECT and MR images.
- 6.18. Display FDG-PET and MR brain images for the same axial slice in MATLAB. Apply edge enhancement methods on both images and compare the definitions of the anatomical structure in PET and MR images.
- 6.19. Compare the resolution, structure details, and image quality of ^{99m}Tc -SPECT and FDG-PET images displayed in Exercises 6.17 and 6.18.

6.6. REFERENCES

1. B. Cassen, L. Curtis, C. Reed, and R. Libby, "Instrumentation for ^{131}I used in medical studies," *Nucleonics*, Vol. 9, pp. 46–48, 1951.
2. H. Anger, "Use of gamma-ray pinhole camera for in-vivo studies," *Nature*, Vol. 170, pp. 200–204, 1952.
3. E. Kuhl and R.Q. Edwards, "Reorganizing data from transverse sections scans using digital processing," *Radiology*, Vol. 91, pp. 975–983, 1968.
4. H. Barrett and W. Swindell, *Radiological Imaging: The Theory of Image Formation, Detection and Processing*, Volumes 1–2, Academic Press, New York, 1981.
5. J.T. Bushberg, J.A. Seibert, E.M. Leidholdt, and J.M. Boone, *The Essentials of Medical Imaging*, Williams & Wilkins, Philadelphia, 1994.
6. Z.H. Cho, J.P. Jones, and M. Singh, *Fundamentals of Medical Imaging*, John Wiley & Sons, New York, 1993.
7. K.K. Shung, M.B. Smith, and B. Tsui, *Principles of Medical Imaging*, Academic Press, San Diego, CA, 1992.
8. G.N. Hounsfield, "A method and apparatus for examination of a body by radiation such as X or gamma radiation," Patent 1283915, The Patent Office, London, 1972.
9. G. Brownell and H.W. Sweet, "Localization of brain tumors," *Nucleonics*, Vol. 11, pp. 40–45, 1953.
10. A. Webb, *Introduction to Biomedical Imaging*, Wiley Interscience-IEEE Press, Hoboken, NJ, 2003.
11. L.S. Zuckier, "Principles of nuclear medicine imaging modalities," in A.P. Dhawan, H.K. Hunag, and D.S. Kim (Eds), *Principal and Advanced Methods in Medical Imaging and Image Analysis*, World Scientific Press, Singapore, pp. 63–98, 2008.
12. M.E. Casey, L. Eriksson, M. Schmand, M. Andreaco, M. Paulus, M. Dahlborn, and R. Nutt, "Investigation of LSO crystals for high spatial resolution positron emission tomography," *IEEE Trans. Nucl. Sci.*, Vol. 44, pp. 1109–1113, 1997.
13. A.P. Dhawan, "A review on biomedical image processing and future trends," *Comput. Methods Programs Biomed.*, Vol. 31, Nos. 3–4, pp. 141–183, 1990.